Please do not adjust margins

COMMUNICATION

Conserved luminal C-terminal domain dynamically controls interdomain communication in sarcolipin

Rodrigo Aguayo-Ortiz, [a] Eli Fernández-de Gortari,[a] and L. Michel Espinoza-Fonseca[a]*

Received 00th January 20xx,
Accepted 00th January 20xx

DOI: 10.1039/x0xx00000x

Sarcolipin (SLN) mediates Ca^{2+} transport and metabolism in muscle through regulation of the Ca^{2+}-ATPase SERCA. SLN has a conserved luminal C-terminal domain whose function remains poorly understood. We used all-atom molecular dynamics simulations of SLN totaling 73 µs to show that the N- and C-terminal domains function in concert, and serial deletions of the C-terminus and phosphorylation affect interdomain communication. We propose the novel hypothesis that the conserved C-terminus is an essential element required for dynamic control of SLN regulatory function.

Sarcolipin (SLN) is a 31-residue membrane protein found in the sarcoplasmic reticulum (SR) of cardiac atrial and skeletal muscle cells.[1] SLN belongs to the family of proteins (which include phospholamban and myoregulin)[2,3] that modulate the activity of the sarcoplasmic reticulum Ca^{2+}-ATPase (SERCA), a ion-motive pump that clears cytosolic Ca^{2+} in muscle cells.[4] SLN plays key roles in muscle cells through regulating Ca^{2+} homeostasis by inhibiting SERCA, and also plays a role in metabolism by inducing unproductive ATPase activity of SERCA and stimulating non-shivering thermogenesis.[5]

SLN consists of three functional domains: (i) an unstructured N-terminus (NT, residues M1-E7) that contains a site for phosphorylation by the calmodulin-dependent protein kinase II (CaMKII) at residue T5;[6] (ii) a transmembrane helix (TM, residues L8-V26) that is important for SERCA binding as well as for self-association;[7,8] and (iii) a conserved luminal C-terminal domain (CT, residues R27-Y31) that protrudes into the SR lumen (**Fig. 1**).[9,10] Experiments and molecular simulation studies have shown that the NT domain plays a primary role in SERCA uncoupling, while the TM domain is necessary for binding and stabilizing the regulatory complex as well as for inhibiting Ca^{2+} affinity.[11,12] However, the role of the highly conserved CT domain (**Fig. S1**, ESI) is more elusive and difficult to interpret. Mutagenesis experiments using co-reconstituted proteoliposomes have suggested that the CT domain is essential for SERCA inhibition,[13] and cell-based studies have shown that deletion of this domain impairs localization and retention in the endoplasmic reticulum (ER).[14] While there is clear evidence for the functional roles of the NT and TM domains of SLN,[5] there is less clear evidence on the functional role of the CT domain. Therefore, we performed µs-long atomistic molecular dynamics (MD) simulations wild-type SLN (SLN_{WT}, residues M1-Y31) and nine serial deletions in the CT domain (SLN_{1-22} through SLN_{1-30}) using Amber ff14SB force field[15] and Amber 18[16]. Methods are described in the Electronic Supporting Information (ESI).

Root-mean-square deviation (RMSD) analysis showed that serial deletion of SLN's CT does not affect the stability of the protein in the µs time scale (**Fig. S2–S11**, ESI). Root-mean-square fluctuation (RMSF) (**Fig. S2–S11**, ESI) and secondary structure (**Fig. S13, ESI**) analyses revealed that the TM domain of SLN is structurally stable in all SLN_{WT} and SLN serial deletion constructs. These analyses imply that deletions in the CT domain, including those beyond the CT domain (i.e., SLN_{1-22} through SLN_{1-26}), do not alter the structural stability of SLN in the conditions used here.

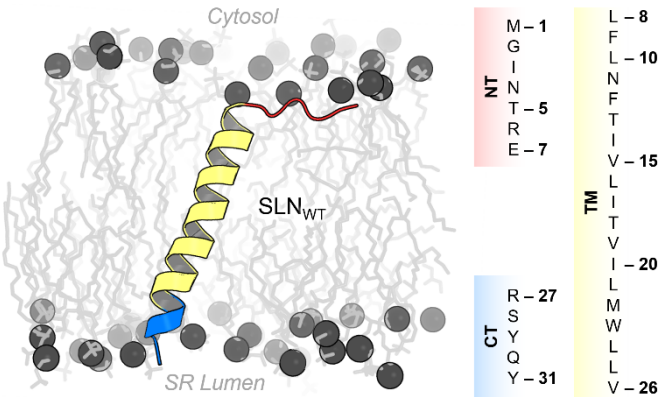

Fig. 1. Structure and amino acid sequence of human SLN. The protein is shown as a ribbon representation and colored according to its functional regions: N-terminus (NT, red), transmembrane helix (TM, yellow), and luminal C-terminal (CT, blue) domains. The headgroup and tails of lipids are shown spheres and sticks, respectively. The columns on the right panel show the amino acid sequence for each functional region of SLN.

[a] Center for Arrhythmia Research, Department of Internal Medicine, Division of Cardiovascular Medicine, University of Michigan, Ann Arbor, MI 48109, USA.

†Electronic Supplementary Information (ESI) available: Materials and Methods, Figures S1-S18, and Supplementary References. See DOI: 10.1039/x0xx00000x

Please do not adjust margins

Please do not adjust margins

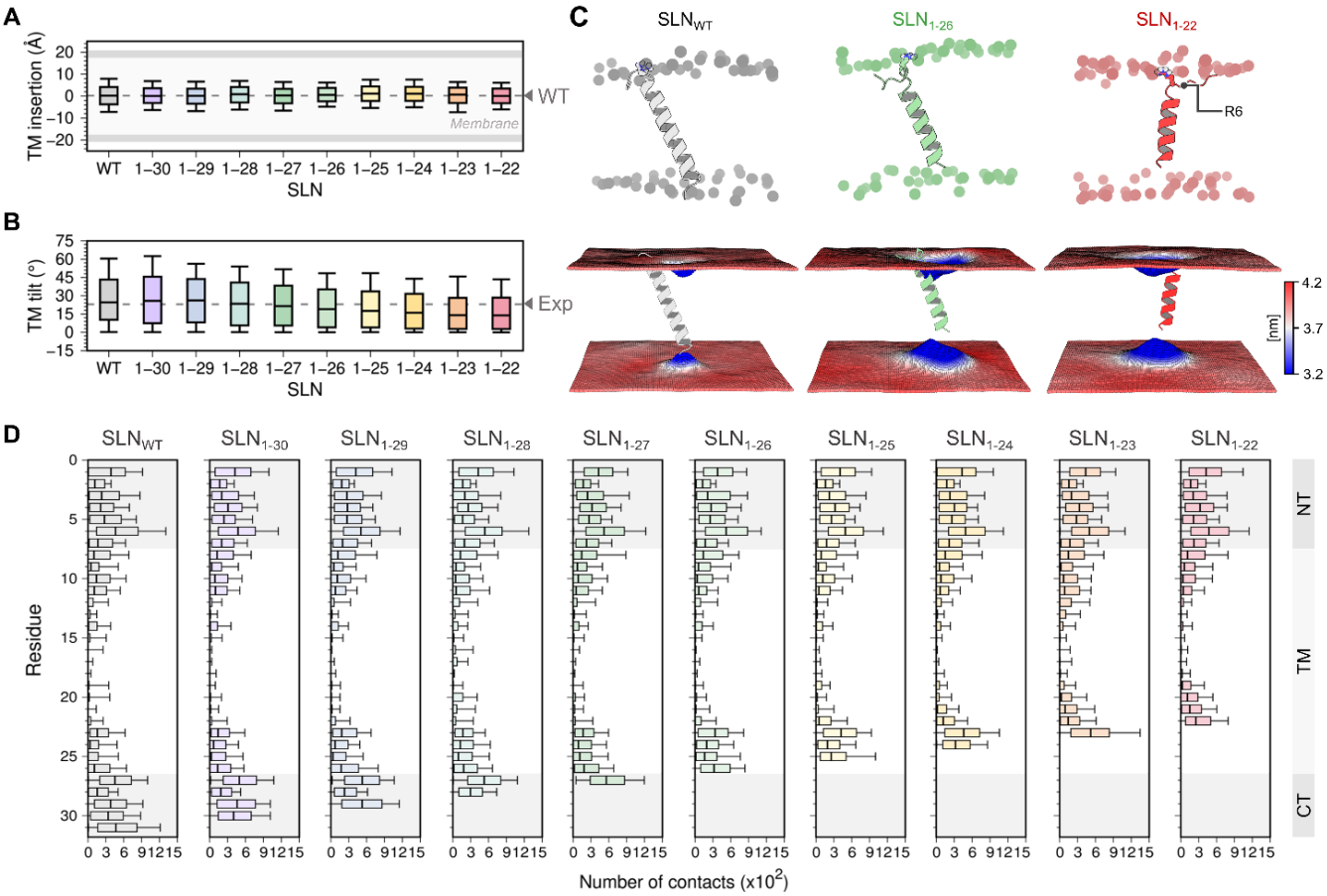

Fig. 2. Orientation and lipid/protein interaction profiles of SLN_{WT} and SLN deletion constructs. (A) Lipid insertion profile relative to the center of mass of both the protein and the lipid bilayer. (B) Tilt angle of the TM domain relative to the membrane normal. The experimental tilt angle of the TM domain is about 23° (Exp., dashed gray line).[10] (C) Representative orientation (*top*) and time averaged local membrane thickness (*bottom*) of the SLN_{WT} (gray, *left*), SLN_{1-26} (green, *center*), and SLN_{1-22} (red, *right*) simulated models. Local membrane property analysis was performed with the *g_lomepro* package.[17] (D) Number of contacts between side chain atoms and lipid headgroup using a cutoff distance of 6.0 Å; shaded gray areas show the location of NT and CT domains of SLN. All box plots show the full range of variation (from minimum to maximum) using 2.5 %, 50.0 %, and 97.5 % quantiles.

After having established that SLN deletion constructs are structurally stable in a lipid environment, we tested the cell-based hypothesis that the CT domain is needed for retention in the lipid bilayer.[14] Lipid insertion analysis showed that incorporation of all SLN deletion constructs in the membrane is similar to that of SLN_{WT} (**Fig. 2A**), indicating that serial deletion of residues in the CT does not induce dissociation of SLN from the membrane. Nevertheless, we found that serial deletion of residues in the CT domain promotes a gradual decrease in the TM tilt angle (**Fig. 2B**) and the local thickness of the lipid bilayer (**Fig. 2C** and **Fig. S12**, ESI).

These findings are intriguing because changes in tilt angle and bilayer induced by SLN deletions are consistent with adaptation to hydrophobic mismatch.[18] This effect correlates with impaired membrane localization and retention upon serial deletions in the CT domain,[14] but we do not observe substantial changes in the insertion profile of SLN deletion constructs (**Fig. 2A**). This apparent contradiction can be reconciled by analyzing the contacts between each residue of SLN and the lipid headgroups (**Fig. 2D**). We focus on residues that play a key role in anchoring and stabilization of proteins in the membrane, such as arginine[19] and tryptophan.[20] We found that in SLN_{WT} as well as SLN deletion constructs SLN_{1-27} through SLN_{1-30}, anchoring residues R6 and R27 (located at the NT and CT domains, respectively) exhibit the highest number of contacts with the lipid headpiece. Serial deletion of CT residues beyond R27 does not induce loss of protein/lipid headpiece contacts involving the NT domain, and the interactions involving anchoring residue R6 remain intact even in the shortest SLN deletion construct SLN_{1-22} (**Fig. 2D**). In the absence of residue R27 in CT domain, we also observed a substantial increase in the number of contacts between residue W23 and the lipid headgroups (**Fig. 2D**), thus indicating that W23 serves as a surrogate anchor in the absence of R27. These findings suggest that while CT residues play a role in SLN preserving normal orientation of SLN in the membrane, the CT domain is not absolutely required for retention and localization. Preservation of the TM domain topology and the presence of native and surrogate anchor residues upon serial deletions in the CT domain help explain experimental evidence showing that SLN deletion constructs are able to localize to the membrane when they are co-expressed with cardiac SERCA.[14]

Closer inspection of the distribution of φ/ψ torsion angles in the NT domain led to the interesting observation that serial

Please do not adjust margins

deletions in the CT induces changes in the backbone dynamics of cytosolic residues I3-E7 (**Fig. S14, ESI**). The distribution of φ/ψ torsion angles indicates that serial deletion of CT residues shifts the equilibrium away from the right-handed α-helix region populated in the SLN_{WT} toward the β-sheet and poly-Pro II regions of the φ/ψ dihedral angle space (**Fig. S14, ESI**). The shift in the φ/ψ torsion angles induced by serial deletions in SLN implies that the CT domain exerts control over the structural dynamics of the NT domain. To test this hypothesis, we performed mutual information analysis[21] of the dihedral distributions to identify correlated motions between the NT and CT domains of SLN. We found that in SLN_{WT}, there is a strong correlation between residues G2-L8 and V26-Q30 (**Fig. 3**). Correlated motions between the CT and NT domains are also observed in SLN_{1-30}, and SLN_{1-29} and to some extent in SLN_{1-28}, but further deletions abolish the ability of the CT domain to communicate with the cytosolic NT domain of SLN (**Fig. 3**). This mechanistic evidence indicates that the CT segment dynamically controls interdomain communication in SLN, and correlates well with experiments showing that deletion of conserved residues R27–Y31 results in loss of function.[13,14]

Intrinsic φ/ψ preferences for individual amino acids which are known to be force-field dependent,[22] so it is possible that the correlated motions between the NT and CT domains is an artifact of the force field and MD engine used here. To rule out this possibility, we performed additional simulations of SLN_{WT}, SLN_{1-26}, and SLN_{1-25} employing the CHARMM36 force field[23] and the NAMD software[24]. We found that SLN constructs simulated with the CHARMM36 force field are structurally stable in the μs timescale, do not dissociate from the membrane upon deletion of the CT domain, and reproduce the decrease in tilt angle and the loss of correlated motions between the NT and CT observed in the simulations performed with the Amber force field (**Fig. S15–S18**, ESI). These findings, which are highly reproducible across force fields, demonstrate that the interdomain communication between the NT and CT domains is an intrinsic functional feature of SLN.

Finally, we asked whether phosphorylation of residue T5, a posttranslational modification that regulates SLN function in the cell,[25] affects interdomain communication in SLN. Therefore, we performed atomistic μs-long MD simulations of SLN phosphorylated at residue T5 (SLN_{pT5}). SLN_{pT5} is structurally stable in the μs timescale (**Fig. S19**, ESI), and that phosphorylation of SLN does not induce substantial changes in membrane insertion (**Fig. 4A**) or tilt of the TM domain (**Fig. 4B**). However, phosphorylation of T5 induces a shift in the φ/ψ torsion angles toward the β-sheet regions of the dihedral angle space (**Fig. 4C**), and also induces a decrease in the correlation between NT and CT domains (**Fig. 4D**). These findings further support our MD-based conclusion that there is dynamic communication between the CT and NT domains, and indicates that the phosphorylation site at residue T5 serves as a switch that modulates interdomain communication to regulate SLN-mediated regulation of SERCA.[26] This mechanistic evidence also supports previous conclusions proposing that the CT and NT are functionally distinct, yet essential domains in the regulation of SERCA.[11,13,27]

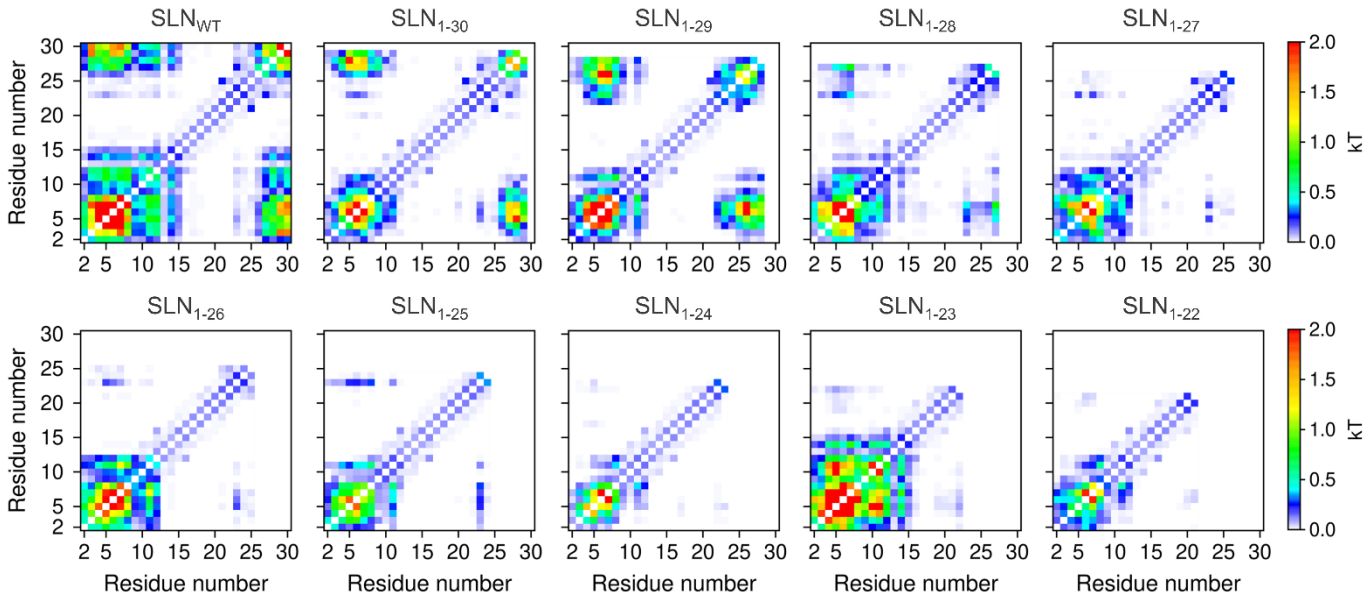

Fig. 3. Mutual information matrix between residues calculated from the trajectories of SLN_{WT} and the nine serial deletion constructs of SLN. Mutual information analysis describes correlations between torsional degrees of freedom from an expansion of the molecular configurational entropy, and is expressed in units of kT.[21] Analysis was performed using the MutInf software package.[21]

Please do not adjust margins

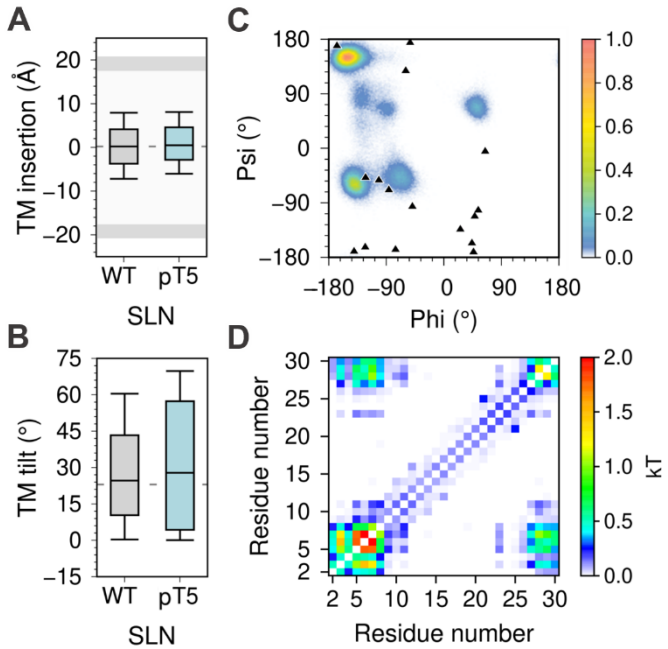

Fig. 4. MD simulations analysis of phosphorylated SLN. (A) membrane insertion and (B) tilt angle of the TM domain in the lipid bilayer. (C) Mutual information matrix between residues calculated from the trajectories of phosphorylated SLN. (D) Dihedral angle distribution of residue T5; the φ/ψ torsion angles calculated from the 16 NMR models of SLN (PDB: 1JDM[9]) are shown as black triangles. All box plots show the full range of variation (from minimum to maximum) using 2.5 %, 50.0 %, and 97.5 % quantiles.

In summary, we used extensive atomistic MD simulations to elucidate the function role of the conserved CT domain of SLN by studying the effect of nine serial deletions in this domain. We find that wild-type SLN and deletion constructs are structurally stable and do not dissociate from the membrane in the µs time scales. However, we found that interdomain communication between the CT and NT domains intrinsic to SLN is abolished upon deletion of the conserved CT domain. This evidence suggests that the CT domain dynamically controls interdomain communication in SLN. This mechanism is further supported by MD simulations of SLN phosphorylated at T5 showing that that there is dynamic communication between the CT and NT domains of SLN. Based on this extensive evidence, we propose the novel hypothesis that the conserved C-terminal domain is an essential element required for dynamic control of SLN regulatory function. These findings have important implications for understanding the molecular mechanisms for interdomain communication in small regulatory proteins, and how this shapes function in the cell.

Conflicts of interest

The authors have no conflicts to declare.

Acknowledgments

This work was supported by the National Institutes of Health grant R01GM120142. This research was supported through computational resources and services provided by Advanced Research Computing at the University of Michigan, Ann Arbor.

Notes and references

1 A. Wawrzynow, J. L. Theibert, C. Murphy, I. Jona, A. Martonosi and J. H. Collins, *Arch. Biochem. Biophys.*, 1992, **298**, 620–623.
2 K. Vogan, *Nat. Genet.*, 2015, **47**, 198–198.
3 D. H. MacLennan and E. G. Kranias, *Nat. Rev. Mol. Cell Biol.*, 2003, **4**, 566–577.
4 N. C. Bal, S. K. Maurya, D. H. Sopariwala, S. K. Sahoo, S. C. Gupta, S. A. Shaikh, M. Pant, L. A. Rowland, S. A. Goonasekera, J. D. Molkentin and M. Periasamy, *Nat. Med.*, 2012, **18**, 1575–1579.
5 M. Pant, N. C. Bal and M. Periasamy, *Trends Endocrinol. Metab.*, 2016, **27**, 881–892.
6 D. M. Anderson, C. A. Makarewich, K. M. Anderson, J. M. Shelton, S. Bezprozvannaya, R. Bassel-Duby and E. N. Olson, *Sci. Signal.*, 2016, **9**, ra119.
7 N. R. DesLauries, B. Svensson, D. D. Thomas and J. M. Autry, *bioRxiv*, 2019, 1–32.
8 J. M. Autry, J. E. Rubin, S. D. Pietrini, D. L. Winters, S. L. Robia and D. D. Thomas, *J. Biol. Chem.*, 2011, **286**, 31697–31706.
9 A. Mascioni, C. Karim, G. Barany, D. D. Thomas and G. Veglia, *Biochemistry*, 2002, **41**, 475–482.
10 J. J. Buffy, N. J. Traaseth, A. Mascioni, P. L. Gor'kov, E. Y. Chekmenev, W. W. Brey and G. Veglia, *Biochemistry*, 2006, **45**, 10939–10946.
11 S. K. Sahoo, S. A. Shaikh, D. H. Sopariwala, N. C. Bal, D. S. Bruhn, W. Kopec, H. Khandelia and M. Periasamy, *J. Biol. Chem.*, 2015, **290**, 14057–14067.
12 A. M. L. Winther, M. Bublitz, J. L. Karlsen, J. V. Møller, J. B. Hansen, P. Nissen and M. J. Buch-Pedersen, *Nature*, 2013, **495**, 265–269.
13 P. A. Gorski, J. P. Glaves, P. Vangheluwe and H. S. Young, *J. Biol. Chem.*, 2013, **288**, 8456–8467.
14 A. O. Gramolini, T. Kislinger, M. Asahi, W. Li, A. Emili and D. H. MacLennan, *Proc. Natl. Acad. Sci. U. S. A.*, 2004, **101**, 16807–16812.
15 J. A. Maier, C. Martinez, K. Kasavajhala, L. Wickstrom, K. E. Hauser and C. Simmerling, *J. Chem. Theory Comput.*, 2015, **11**, 3696–3713.
16 D. A. Case, R. M. Betz, W. Botello-Smith, D. S. Cerutti, T. E. Cheatham III, T. A. Darden, R. E. Duke, T. J. Giese, H. Gohlke, A. W. Goetz, N. Homeyer, S. Izadi, P. Janowski, J. Kaus, A. Kovalenko, T. S. Lee, S. LeGrand, P. Li, C. Lin, T. Luchko, R. Luo, B. Madej, D. Mermelstein, K. M. Merz, G. Monard, H. Nguyen, H. T. Nguyen, I. Omelyan, A. Onufriev, D. R. Roe, A. Roitberg, C. Sagui, C. L. Simmerling, J. Swails, R. C. Walker, J. Wang, R. M. Wolf, X. Wu, L. Xiao, D. M. York and P. A. Kollman, 2018, University of California, San Francisco.

Please do not adjust margins

Please do not adjust margins

17 V. Gapsys, B. L. De Groot and R. Briones, *J. Comput. Aided. Mol. Des.*, 2013, **27**, 845–858.

18 M. R. R. de Planque, E. Goormaghtigh, D. V. Greathouse, R. E. Koeppe, J. A. W. Kruijtzer, R. M. J. Liskamp, B. de Kruijff and J. A. Killian, *Biochemistry*, 2001, **40**, 5000–5010.

19 M. B. Ulmschneider, J. P. Ulmschneider, J. A. Freites, G. von Heijne, D. J. Tobias and S. H. White, *Eur. Biophys. J.*, 2017, **46**, 627–637.

20 A. J. De Jesus and T. W. Allen, *Biochim. Biophys. Acta - Biomembr.*, 2013, **1828**, 864–876.

21 C. L. McClendon, G. Friedland, D. L. Mobley, H. Amirkhani and M. P. Jacobson, *J. Chem. Theory Comput.*, 2009, **5**, 2486–2502.

22 J. Vymětal and J. Vondrášek, *J. Chem. Theory Comput.*, 2013, **9**, 441–451.

23 J. Huang and A. D. M. Jr, *J. Comput. Chem.*, 2013, **34**, 2135–2145.

24 J. C. Phillips, R. Braun, W. Wang, J. Gumbart, E. Tajkhorshid, E. Villa, C. Chipot, R. D. Skeel, L. Kalé and K. Schulten, *J. Comput. Chem.*, 2005, **26**, 1781–1802.

25 P. Bhupathy, G. J. Babu, M. Ito and M. Periasamy, *J. Mol. Cell. Cardiol.*, 2009, **47**, 723–729.

26 P. Bhupathy, G. J. Babu, M. Ito and M. Periasamy, *J. Mol. Cell. Cardiol.*, 2009, **47**, 723–729.

27 J. M. Autry, D. D. Thomas and L. M. Espinoza-Fonseca, *Biochemistry*, 2016, **55**, 6083–6086.

Please do not adjust margins